REPORT DOCUMENTATION PAGE

Form Approved
OMB No. 0704-0188

1. REPORT DATE *(DD-MM-YYYY)*	**2. REPORT TYPE**	**3. DATES COVERED** *(From - To)*
17-08-2006	Journal Article PREPRINT	2006

4. TITLE AND SUBTITLE
Inertially Stabilized Platforms for Precision Pointing
Applications to directed-energy weapons and space-based lasers (PREPRINT)

5a. CONTRACT NUMBER

5b. GRANT NUMBER

5c. PROGRAM ELEMENT NUMBER

6. AUTHOR(S)
J. Negro, S. Griffin

5d. PROJECT NUMBER

5e. TASK NUMBER

5f. WORK UNIT NUMBER

7. PERFORMING ORGANIZATION NAME(S) AND ADDRESS(ES)

Boeing-SVS Inc
4411 The 25 Way NE
Albuquerque, NM 87109

8. PERFORMING ORGANIZATION REPORT NUMBER

9. SPONSORING / MONITORING AGENCY NAME(S) AND ADDRESS(ES)

Air Force Research Laboratory
Space Vehicles Directorate
3550 Aberdeen Ave SE
Kirtland AFB, NM 87117-5776

10. SPONSOR/MONITOR'S ACRONYM(S)
AFRL/VSSV

11. SPONSOR/MONITOR'S REPORT NUMBER(S)
AFRL-VS-PS-JA-2006-1017

12. DISTRIBUTION / AVAILABILITY STATEMENT
Approved for public release; distribution is unlimited. (Clearance #VS06-0383)

13. SUPPLEMENTARY NOTES
Submitted for publication in the IEEE Magazine

Government Purpose Rights

14. ABSTRACT

Tactical and space-based high-energy-laser weapon systems present interesting challenges for precision line-of-sight control. Sub-μradᵢ pointing accuracies are required against dynamic targets. In addition, absolute pointing and inertial angular-rate measurements are required to support mission requirements. This article addresses directed-energy-weapon (DEW) precision pointing requirements and implementation alternatives in the context of strapdown and stable-platform inertial-reference technologies. Prior work has addressed details of stable platform design and test results. The contributions of the present article include the broader issues of DEW requirements drivers, integration of the stabilization system with the remaining optical system, and design tradeoffs between stable-platform and strapdown stabilization mechanizations.

15. SUBJECT TERMS
DEW, Precision Pointing, Stabilized Platforms, Directed Energy Weapon, Strapdown

16. SECURITY CLASSIFICATION OF:			**17. LIMITATION OF ABSTRACT**	**18. NUMBER OF PAGES**	**19a. NAME OF RESPONSIBLE PERSON**
a. REPORT	**b. ABSTRACT**	**c. THIS PAGE**			Benjamin K Henderson
Unclassified	Unclassified	Unclassified	Unlimited	55	**19b. TELEPHONE NUMBER** *(include area code)* 505-853-6712

Inertially Stabilized Platforms for Precision Pointing

Applications to directed-energy weapons and space-based lasers

J. Negro and S. Griffin

Tactical and space-based high-energy-laser weapon systems present interesting challenges for precision line-of-sight control. Sub-μraḍ pointing accuracies are required against dynamic targets. In addition, absolute pointing and inertial angular-rate measurements are required to support mission requirements. This article addresses directed-energy-weapon (DEW) precision pointing requirements and implementation alternatives in the context of strapdown and stable-platform inertial-reference technologies. Prior work [1] has addressed details of stable platform design and test results. The contributions of the present article include the broader issues of DEW requirements drivers, integration of the stabilization system with the remaining optical system, and design tradeoffs between stable-platform and strapdown stabilization mechanizations.

Gyro-stabilized pointing controls have been implemented for over 60 years. The earliest applications provided lead compensation for anti-aircraft guns. Most gyro-stabilized platform applications are for inertial navigation systems in which gyros provide measurements to maintain an accurate orientation knowledge of an accelerometer triad, as required for accurate navigation solutions. Another application includes gyro-stabilized gimbal pointing systems, used for camera or electro-optical sensor-imaging applications.

With the advent of lasers in 1959, the need arose to precisely point these devices. Laser pointing and tracking-system development occurred rapidly in the 1970s with the production of ground-based, sea-based, and airborne DEW pointing systems under programs sponsored by the Air Force Weapons Laboratory (now the Air Force Research Laboratory) and the Navy Sea Systems Command – PMS 405. The early systems, designed and built by the Hughes Aircraft Company, were based on an approach in which telescopes were mounted on gimbals and stabilized using gyros mounted directly to the telescope. This approach is called an “on-gimbal stabilized telescope” approach. By the mid 1970s larger telescope apertures were of interest and by the early 1980s the prospect of viable space-based laser systems provided a key impetus to the formation of the Strategic Defense Initiative Organization, now known as the Missile Defense Agency (MDA). Basing lasers in space, despite issues associated with deploying sophisticated hardware, has the advantages of negligible degradation of laser propagation due to the atmosphere as well as fewer limitations on the deployment of large optics that enhance capability at long ranges.

A key laser system figure-of-merit is λ/D, the ratio of wavelength to telescope aperture diameter. All things being equal (especially total laser power), the smaller λ/D is, the better. Smaller λ/D implies a smaller beam-spot size on target, which requires correspondingly smaller line-of-sight (LOS) jitter to take advantage of the spot size. Figure 1 plots λ/D as a function of telescope diameter for several laser wavelengths ranging from excimer lasers in the UV to CO_2 lasers in the mid-IR. Although the 10.6-μm wavelength associated with CO_2 lasers is not attractive for space, it is shown here for reference purposes since this wavelength was used for early ground and airborne laser systems. The aperture diameters shown in Figure 1 range from a few tens of centimeters for terrestrial applications to 10 m for space applications.

Required pointing accuracies scale directly with λ/D. LOS pointing accuracies range from approximately 20 μrad for 50-cm CO_2 laser systems (long wavelength; small aperture) to approximately 40 nrad for 10-m excimer laser systems (short wavelength; large aperture). More practical space-based laser systems have sub-μrad root-mean-square (rms) jitter pointing requirements. These requirements are more stressing than those of any other application. While rms LOS jitter is a key requirement for space-based laser systems, it is not the only requirement. Additional LOS requirements related to the design of a DEW pointing system are presented in the next section.

Unique Directed Energy Requirements

Large-aperture space-based laser pointing systems present numerous challenges to the LOS pointing system designer. One significant issue is how to optically integrate an inertial LOS sensor suite into a large-aperture optical system. Other important questions relate to dynamic target acquisition with narrow field-of-view (FOV) sensors and how to implement point-ahead functions. These three issues, namely, optical integration, absolute pointing, and point ahead, are addressed in the following subsections. Unique requirements of inertial instruments for precision pointing applications are also discussed in a later section.

Optical Integration

Early DEW pointing systems for terrestrial applications were based on the on-gimbal telescope configuration. Here, an on-gimbal telescope is stabilized with a strapdown gyro tip/tilt diad to measure angular motion in the two coordinate axes perpendicular to the nominal telescope boresight axis. These measurements are fed back to a rate-loop gimbal controller. High bandwidth inertial measurements can be useful in implementing high bandwidth gimbal-rate stabilization loops or for implementing accurate, high-bandwidth beam alignment controls. The alignment subsystem maintains accurate alignment of multiple optical components between the off-gimbal laser and the on-gimbal transmitting aperture and can be “offset pointed” to correct for telescope control errors.

The alignment subsystem plays a crucial role in the integration of small stable platforms with large-aperture pointing systems. In this configuration, gyro inertial sensors are mounted on

a small[1] stable platform that has two degrees-of-freedom, namely, tip/tilt with respect to its base. The platform tip/tilt angles are servo controlled with pairs of linear actuators that torque the platform about a central pivot hinge. Gyro signals are used to implement a rate loop. The additional degrees-of-freedom of the stable platform to better isolate high-frequency gimbal vibrations. The gyro servo control provides excellent isolation at low frequency, while the natural moment-of-inertia provides isolation at high frequency.

Absolute Pointing

DEW systems must point toward targets with μradianฺ and sub-μradianฺ accuracies. Although imaging sensors are used to make these measurements, because of detector array size and processing limitations, the total FOVs of these sensors are limited. Even with a cascade of multiple sensors with telescoping FOVs, the initial acquisition sensor has a FOV of only a degree or so. Thus, the DEW LOS system must maintain absolute pointing knowledge to support target acquisition given target-coordinate handover information from an offboard ancillary surveillance sensor. Given surveillance tracking errors and the desire for a high probability (>98%) that the target is within the DEW initial acquisition sensor FOV, the DEW attitude control system must maintain attitude knowledge of better than a few milli-radians rms. While this mission need leads to gyro requirements on the order of 0.5°/h, which is not particularly stressing, it does impose the need for full 3D attitude computation and the need for star trackers to provide a dc pointing reference.

[1] Small here is with respect to the telescope aperture. Generally, the size only needs to be large enough to accommodate the gyro sensors and the alignment probe beam source.

Point Ahead

While the photons of DEW systems fly at the speed of light, the large target ranges associated with future space systems correspond to significant times of flight. Thus, the finite propagation times in concert with target relative angular rates lead to the requirement to point ahead of the tracker-measured target location. The point-ahead angle is given by the relative angular rate times the round-trip propagation time, that is,

$$\phi_{PA} = \dot{\theta} \cdot t_p = \dot{\theta} \cdot \frac{2R}{c}, \tag{1}$$

where ϕ_{PA} is the required point-ahead angle, $\dot{\theta}$ is the relative angular rate, R is the target range, and *c* is the speed of light. Point-ahead angles of up to 50 μrad are reasonable for many missions. Since the point-ahead angle scales linearly with angle-rate measurement, the inertial sensors must provide this measurement to an accuracy of about 1 part in 100 to ensure that overall sub-μraḍ pointing accuracy is achieved. Like the gyro bias stability, this angular rate measurement precision is not particularly stressing for gyro technology, but it does necessitate accurate conversion from gyro-measurement coordinates to optical-LOS coordinates. Accurate implementation of point ahead also requires precise offset pointing of the optical beam-train alignment system.

Ultra Noise Jitter and Dynamic Range Requirements

Stable-platform gyros provide both sub-μraḍ angle references and angle-rate measurements for acquisition slew. The need to meet both of these requirements can stress the inertial instrument dynamic-range requirements. For example, at an angular resolution of 0.1 μradiaṇ, an output data rate of 1 MHz is required for angular rates of 0.1 radian/s or more. While dual-range instruments have been considered, none are available for precision-pointing applications. Indeed, almost all of the available inertial instruments have been developed for navigation, not pointing applications.

Implementation Trades and Alternative Configurations

This section addresses design tradeoffs between alternative pointing system configurations. Two quite distinct alternative configurations, the stable-platform and the strapdown pointing and stabilization implementation architectures for large aperture space-to-space optical systems are described. Following the alternative architecture discussion, the beam control alignment subsystem features common to both these architectures are described. Then the subsystem features which are distinct between these architectures are described.

These alternative approaches are compared on the basis of performance, cost, and system complexity as the primary evaluation criteria. The performance trades are conducted with the stipulation that the jitter performance goals must be met by the candidate system so that this criterion does not become a major driver unless one architecture cannot meet performance requirements. The cost and complexity trades are addressed relatively and qualitatively. In many applications, both the strapdown and stabilized-platform approaches are technically viable mechanizations for LOS stabilization. The choice of mechanization depends primarily on the pointing accuracies required and the magnitudes of the base motion angular vibration that exists in the system. Generally, it is argued that the simpler implementation makes the strapdown mechanization the superior approach provided that this approach can meet the overall performance goals. In some applications, however, the desired performance cannot be achieved with the strapdown approach, because the sensors cannot accommodate the large bandwidth and large dynamic range of the underlying disturbance base motion. These applications can be handled only by the stabilized-platform approach which gives superior performance to that attainable with strapdown mechanizations.

A necessary condition for selecting an inertial reference approach is that it meet jitter performance requirements. Jitter performance must be achieved in the prescribed base motion environment, that is, in the presence of platform base motion. The angular base motion is of obvious concern, though any significant disturbance must be evaluated. Linear motion may be an issue because of the way it couples into angular motion of the system and the way it might couple as measurement errors in the sensors. Various base-motion models have been considered. Unlike astronomical telescopes such as Hubble and Chandra, for which the attitude-control actuators are the dominant high-frequency jitter contributor, space-based DEW concepts have significant disturbances associated with the laser, typically gas and fluid flow associated with the laser beam generation and cooling system. These broadband disturbances make precision LOS jitter control more challenging for space-based DEW systems. Other potential mechanical disturbance sources include fluid flow and slosh, actuator reaction torques, and cryogenic cooler pump disturbances any of which may induce jitter into the optical components in a beam path as well as contribute to base motion disturbance. In addition, because the attitude slew rates of DEWs are significantly higher than those required for astronomical space telescopes, the disturbances associated with DEW attitude actuators are also larger. As expected, the results depend on the high-frequency base-motion content, and this sensitivity is shown in the comparison of results for the base-motion models. The methodology of this study can be applied to specific application cases whenever detailed base-motion models exist.

Figure 2 shows the modeled angular base-motion random vibration. These disturbance inputs are used to compare the performance of strapdown and stabilized-platform jitter-

suppression systems. These spectra have base-motion rms angles ranging from 15 to 53 μrad. These values are typical for satellite electro-optical pointing applications and also might represent a low-disturbance tactical application, although tactical DEW applications generally have more severe base-motion environments as shown in Figure 3.

If both strapdown and stabilized-platform approaches meet performance criteria and have comparable costs, then the less-complex system is preferred. Often the less complex system has lower cost, but the complexity factor is included to capture the additional work required for integrating, checking out, testing, and maintaining the more complex approach. Cost and complexity issues primarily become drivers whenever the strapdown implementation is being stressed to become performance competitive with the stabilized-platform approach. In these cases, sophisticated inertial instruments (high-bandwidth, low-noise inertial instruments), signal processing (broadband dynamic match) and precision optical controls (large-dynamic-range optical-alignment sensors) are required to achieve satisfactory performance in the strapdown approach.

Stabilized Platform Description

The stabilized platform approach entails a two-axis tip-tilt platform with integrally mounted inertial angle sensors and an alignment probe beam. The alignment probe beam is propagated through the optical train to an alignment sensor that detects the angular misalignment of the probe beam with respect to an alignment fiducial reference. The sensor error signals drive an alignment servo control loop to null the sensor-alignment error. The platform is articulated (a

few milliradians travel, maximum) relative to its gimbal mounted base with push-pull voice-coil actuators. For terrestrial applications, the stabilized IRU is assumed to be mounted on a multi-axis gimbal to provide large-angle field-of-regard coverage. For space-based applications, the large-angle coverage is provided by the spacecraft attitude control system.

The stabilized platform control architecture is depicted in Figure 4. This configuration is explicit for the case in which the beam director telescope is gimbaled with respect to a host platform. The configuration diagram for an optical alignment loop needed to null the beam path errors is depicted in Figure 5. The optical path shows dual-mirror actuators. A fast steering mirror (FSM) controls jitter, while a beam walk mirror (BWM) controls beam translation. Beam jitter and beam walk alignment sensors control these mirror actuators in a feedback servo control fashion.

Tracker measurements of the target pointing error, or inertial angle commands, control the stable platform to point it toward the target. The platform angles with respect to its base are then used to point the host platform as a follower control system.

Strapdown Description

In the strapdown approach, the inertial sensors are hard mounted to the beam expander telescope directly adjacent to an alignment reference. The angular motion of the reference surface is measured, and a correction signal is applied to the alignment loop to correct the error.

Often this correction is done only in a high-pass (no DC) context, because of the errors inherent in measuring and correcting DC bias error with inertial only systems. The key elements of a strapdown stabilization approach are an alignment system, including reference beam, beam sensor, and a reference surface indicative of the telescope output optical axis. Also, there is an inertial sensor measurement of the reference surface motion.

The strapdown control architecture diagram is depicted in Figure 6. This configuration is explicit for the case in which the inertial angle sensors are strapped to the telescope. The gyro measured angular rate (or delta inertial angle) is used to implement a telescope rate stabilization control loop. Other details of the control architecture require examination of the optical alignment system. The alignment system for a strapdown implementation is shown in Figure 7. The alignment system includes jitter alignment and beam walk sensors, just as it does for the stabilized platform mechanization. As shown in Figure 7, high-rate data processing is required to implement the calibration, coordinate rotation, and dynamic compensation computations for implementing the alignment system pointing offsets which correct telescope pointing error.

In addition, FSM (and BWM) position pickoff signals are used to generate telescope pointing commands to the gimbal motor drives as shown in Figure 7, or to the spacecraft attitude control system, as it would be in a space-based application.

Many types of alignment references can be used. Two common types are a reference flat and a reference probe beam. The reference flat approach defines output reference of a two-pass autocollimator. An alignment beam is projected from the beam control optical bench. This

reference beam is reflected by the reference flat and propagates back to the optical bench where it is sensed. The arrival angle of the retro beam with respect to the outgoing beam is a measure of misalignment. This approach has been used on a variety of large-aperture precision-pointing telescopes.

An alternative implementation scheme is to replace the reference flat with a probe beam source. The probe beam source is rigidly attached to the beam expander transmitting telescope. Simply stated, this alignment system configuration is identical to that of the stabilized platform in which the platform angle, relative to the base, is held fixed (strapped down). Operation of the alignment system makes the optical axis aligned with the reference beam. High-frequency inertial angle motion of the reference beam can be measured with the collocated inertial sensors. The high-frequency error of this angle motion is due to gimbal and probe beam mechanical mounting jitter, which can be corrected by offsetting the alignment sensor null point by the measured inertial misalignment measurement. This process entails careful match of the scale factors of the inertial and optical sensors and coordinate transformations to account for the coordinate transformation (rotation about the optical axis) between inertial sensor coordinates where the errors are measured and alignment sensor coordinates where the errors are offset.

System Commonalities

The two inertial stabilization approaches have many commonalties. They both depend upon an optical probe beam that is propagated through the optical train to an alignment sensor

where optical train alignment error is sensed. The probe beam and the alignment actuators are basically identical in both approaches. The other components have significant differences, as explained in the System Distinctions section below.

Alignment Probe Beam

The probe beams are identical. Beam diameter, beam optical power, beam jitter stability, and beam optical quality are the same in both inertial stabilization approaches. Care must be taken in these jitter suppression approaches to minimize errors due to beam vignetting, beam walk on the optical surfaces, and field-distortion errors. These effects must be considered in both approaches, although the details will differ due to the different propagation paths of the beam through the system.

A collimated optical alignment probe beam is propagated through the optical beam train to provide an end-to-end alignment reference from the beam source to the beam detector. Once aligned, the alignment sensor has a calibrated null point. Thereafter, the motion (or misalignment) of any optical element in the beam path generates an alignment sensor error signal. The error signal is used in a servo control loop to drive a fast steering mirror to null the error. The residual error after this process is that due to alignment sensor and probe beam jitter, actuator noise (usually small), and the limited capability of the servo control to null alignment disturbances due to their amplitudes or spectra. Important performance characteristics of the alignment probe beam are its wavelength, optical power, optical wavefront quality, and beam

jitter. Beam jitter is a direct error source. The optical wavefront quality affects the far-field point spread function and the capability of the angle sensor to measure the alignment beam spot position, and hence the alignment beam angle, in the alignment sensor. Finally, the beam power impacts the sensor signal-to-noise ratio (SNR) and the sensor noise equivalent angle.

Alignment Actuators

Once an angular error in the beam train has been sensed, it needs to be corrected. Steering mirrors are typically used for this application. Often these are designated Fast Steering Mirrors (FSMs) to distinguish them from low-bandwidth steerable mirrors used for static alignment applications. FSMs typically have tip-tilt control and are driven by push-pull actuator pairs. Often they have position sensors indicating the off-null angular position of the mirror.

The alignment actuators requirements are also identical in both stabilized platform and strapdown beam control configuration. The gimbal and beam optical path errors, relative to the target LOS, are the same in both cases. Hence, the actuators required to null these error should have the same control dynamic range and bandwidth requirements to achieve the same overall alignment performance.

System Distinctions

Besides the obvious distinction that the strapdown stabilization approach does not have a stabilized platform with its associated flex pivot, drive actuators, and position pickoff signals, there are differences in the performance requirements of the common components, specifically the inertial sensors and the alignment sensors, which are necessary for the strapdown and the stabilized inertial stabilization schemes to have comparable performance. Each of these components is described along with their features which are distinguished between the two beam control architectures. The inertial platform, the inertial sensor and the alignment components are described in the following subsections.

Platform

A mechanical platform serves as the mounting assembly for the inertial instruments and the optical probe beam. This mechanical assembly holds the inertial instruments and the IRU probe beam in alignment with respect to each other. The platform is articulated in two axes (tip-tilt) using high-bandwidth voice-coil actuators. These actuators operate in push-pull pairs to impart a torque on the platform in reaction to the base. The torque angularly accelerates the platform, and is used to control inertial angular rate and, hence, the inertial attitude [i.e. the pointing direction / line-of-sight (LOS**)]**. Precision linear pickoff sensors, operated differentially, measure the relative displacement of the platform, with respect to the base, on opposite ends of a diameter passing through the platform flex pivot. These differential linear

sensors give an output proportional to the angle of the platform with respect to the base. A precision flex pivot allows the platform high compliance (low stiffness) motion in 2 degrees-of-freedom (tip-tilt) while providing low compliance in the other degrees-of-freedom.

A significant advantage of the stabilized platform approach compared to the strapdown approach is the broadband jitter immunity that it provides, as shown in Figure 8, which depicts the transfer function from base-motion input angle to platform angle. This transfer function is typical of the base-motion error-rejection characteristics typical of stabilized platforms. Note that the platform angle is not the angle with respect to its base, rather is measured with respect to an inertial reference. Since the platform angle represents a system pointing error, greater rejection corresponds to better system performance. The platform rejection at low frequency is provided by the closed-loop servo of the platform angle around the gyro sensors. The high-frequency attenuation is provided by the inherent moment-of-inertia of the platform, which requires high disturbance torques to accelerate the platform at high frequency. This high-frequency disturbance rejection gives the stabilized platform approach a significant advantage over strapdown approaches. Of course, this advantage is only realized in the presence of high-frequency disturbances.

Inertial Sensor Requirements

Both implementation concepts require inertial sensors to measure the inertial angle error. The sensor requirements for these sensors, however, can be substantially different. In both cases

the sensors require good low angle noise. The bandwidth of the angle measurements might be higher for the strapdown implementation, however, so its noise performance may be more difficult to achieve. Therefore, the bandwidth over which the noise is important is higher for the strapdown implementation. Furthermore for the strapdown architecture, the sensor's precise gain and phase characteristic must be well calibrated so that the inertial sensor measurement is correctly commanded as an offset set point to the alignment servo loop.

Various inertial instruments are employed in inertial attitude stabilization. Both low-bandwidth gyros and high-bandwidth angle sensors are typically used. Until the mid 1980's the dry-tuned gyros (DTG) were the instruments of choice. These mechanical instruments have mechanical sensing elements with large moments-of-inertia generated by a spinning mass. The mass is inertially stabilized since significant torques are required to rotate the spinning mass. The motion of the case relative to the mass indicates angle change. The instruments can also be operated in a torque-rebalance mode in which precisely calibrated torques are electromechanically applied to the spinning mass. With the known applied torque, and the known mass moment-of-inertia, the mass precesses at a constant angular rate given by the relationship $\omega = T/H.$ in which ω is the angular rate, T is the applied torque and H is the momentum of the spinning reference mass. If this rate matches the inertial rate of the gyro case, then no relative angle is generated and the sensor output is zero. The Singer-Kearfott MODIIe/s, which is a dry-tuned gyro (DTG), is used in the Inertial Pseudo-Star Reference Unit (IPSRU) built by Draper Laboratory. The IPSRU, which is the most precise inertial stabilization system built to date, is shown in Figure 9.

Alternative gyro instruments used in platform or strapdown configurations include ring laser gyros (RLGs), zero-lock laser gyros (ZLGs), fiber optic gyros (FOGS), and hemispherical resonant gyros (HRGs). RLGs, ZLGs, and FOGS operate on the rotation-dependent differential properties of light propagation in a closed circular path, known as the Sagnac effect. HRGs depend on the inertial properties of mechanical resonant mode shapes set up in a quartz wine glass. All inertial instruments have error mechanisms that limit their performance. While the characteristics of these errors are different for different instruments, the principal gyro-error mechanisms are those shown in **Error! Reference source not found.**. The higher-order rate errors are of no consequence for jitter, but are crucial for absolute pointing accuracy. Instrument bandwidth is another important characteristic. FOGs tend to have the highest available bandwidths, while mechanical gyros tend to have the lowest bandwidths. Typical bandwidths range from 10-200 Hz.

Error State Name	**Symbol**	**Uncertainty (rms)**
Gyro angle error	σ_N	.05 – 1.0 μrad
Gyro angle random walk	σ_{ARW}	See Reference 1
Gyro bias stability	$\delta\underline{b}$	2.4×10^{-8} rad/sec
Gyro bias asymmetry	$\delta\underline{nl}_1$	3 ppm
Gyro scale factor	$\delta\underline{S}$	5 ppm
Gyro rate-squared error	$\delta\underline{nl}_2$	0
Gyro rate-cubed error	$\delta\underline{nl}_3$	0
Gyro misalignment	$\underline{\gamma}^{Gm}$	10^{-5}
Gyro non-orthogality	$\underline{\gamma}^{Go}$	10^{-5}

Table 1 Error State Random Characteristics.

All gyros have bandwidth limits. Generally, the mechanical gyros, with the exception of the HRG, have bandwidths on the order of a few tens of Hz. The HRG and optical instruments can be designed to have bandwidths of several hundred Hz. Care must be taken in using the high-bandwidth instruments, since their larger bandwidth correspond to larger noise-equivalent angle noises. However, gyro bandwidth is needed so that the dynamic error of the instrument is small. Figure 10 shows this bandwidth error as a fraction of the input amplitude. Even at frequencies as high as $1/10^{th}$ the bandwidth, a 10% amplitude error occurs. Exact results depend on the gyro transfer function. These errors are especially important for strapdown applications, even if blended inertial sensor outputs are used.

For the strapdown architecture, inertial instruments are required to measure the jitter of the alignment reference and provide offset correction signals to the alignment servo controls. This open loop correction places stringent requirements on the inertial measurements. First of all, the instruments see larger higher-frequency input error signals since there is no base disturbance attenuation mechanism as is provided by the platform isolation. In the strapdown case, gyro (and other inertial sensor) measurements need to be sufficiently broadband that all significant base angle motion is measured. That bandwidth must be such that the residual base motion error above the instrument bandwidth is an acceptable error in an overall error budget. Hence, higher bandwidth more precise inertial instruments are required for the strapdown approach. This inertial sensor bandwidth requirement and the need to precisely and dynamically match the gyro inertial angle measurement and the optical pointing offset make strapdown implementations unattractive in all but the low disturbance cases.

Two different types of high-bandwidth angle sensors have been used, the Systron Donner (now BEI) Angle Displacement Sensor (ADS), and the ATA Sensors Magneto-hydro-dynamic (MHD) angle rate sensor, in particular the ARS-12. Both sensors have good low-noise performance (< 50 nrad). Neither instrument has a dc response (~ 2-Hz break frequency) and care must be taken with respect to instrument response to input transients and to saturation. Figure 11 shows the noise spectra for a variety of inertial instruments. This data represents direct measurements obtained by the Draper Laboratory [1].

Alignment Sensor Requirements

Just as is the case for the inertial sensors, both implementations require good low-noise performance from the alignment sensor. The strapdown implementation poses additional requirements on the sensor for increased dynamic range and superior scale factor stability and linearity.

The collimated alignment probe beam is focused on a detector where the beam 2-D displacement is proportional to angle in the tip-tilt axes. Thus, the detector processing problem is to accurately measure the position of the focused probe beam. Position Sensitive Detectors (PSDs) and Charge Coupled Devices (CCDs) have typically been used for this application as well as quad cells and multiple distinct sensors. The key alignment sensor parameters are noise (and noise equivalent angle), sensitivity, and stability (null point, linearity).

For the stabilized platform architecture, a single sensor null-point exists. The alignment actuators are driven to achieve small error with respect to this null.

For the strapdown case, the desired null point for alignment dynamically varies with the inertial measurements of the probe beam source jitter. These measurements must accurately offset those of the alignment sensor to establish an overall system alignment null. Because the alignment sensor is operated off null, its linearity and scale factor must be accurately known to provide accurate control offsets. Dynamic ranges to angle noise ratios as large as 10^5 may be required in some applications. These requirements are unique to the strapdown case.

Figure 12 and Figure 13 show how the misalignment error due to inertial motion of the beam director telescope is sensed. Figure 12 shows the stabilized platform case while Figure 13 shows the strapdown case. Both aligned and misaligned configurations are shown in each instance.

In the stabilized platform case (Figure 12) the inertial motion of the telescope does not cause a stable platform error, because the platform is actively stabilized. This alignment error is sensed by the alignment probe beam sensor and corrected at high bandwidth.

In the strapdown case, inertial motion of the telescope also moves the strapdown instruments, thereby generating an inertial angle error. However, there is no corresponding alignment error. The inertial angle sensors, by means of gimbal control, will act to minimize the

pointing error, subject to the bandwidth limitations of the gimbal servo. Since the gimbal bandwidth is generally low in comparison to the disturbance induced error, a highly effective bandwidth control must be used and is achieved by using the measured inertial angle error from the strapdown inertial sensors to offset the alignment servo in order to correct the overall beam pointing error induced by the telescope motion.

The inertial sensor provides a dynamic offset command to the alignment loop. Ideally, the alignment loop should follow this command input precisely. In the strapdown implementation, there is no sensor that directly measures the alignment error with respect to inertial space at high bandwidth. The outputs of the inertial sensors (gyros) and the alignment sensors must be electronically combined to effectively achieve the desired sensor error signal. Because these signals are dynamically combined, the optical alignment sensor must generate a signal of equal magnitude and opposite polarity to that of the inertial sensors. The magnitude of this offset is the maximum inertial error that can occur, which is substantially larger than the stabilization error. Therefore, the optical alignment sensor must have a dynamic range determined by the inertial errors, not just the alignment error.

Also, the scale factor of both the gyro inertial angle measurements and the optical alignment sensor must be well matched dynamically. Mismatches in sensor scale factors lead to errors proportional to the input angle magnitude.

Software

The primary difference in software development requirements between the stabilized platform and the strapdown implementations relates to software for the servo control of the platform versus software required to process and transform the inertial sensor measurements.

The software functions required to implement the stabilized platform servo controller are at a significantly lower (10x) bandwidth than those of the alignment loop. Hence, timing and data calculations are more difficult. Figure 7 shows the inertial sensor calculations (error compensation), the coordinate rotation (due to image rotation through the gimbal coudé path), and dynamic compensation (to match sensor and control frequency domain effects). The differences are described in Table 2 below.

Function	Software Implications
Platform Servo Control	
Pickoff Signal Processing	Perform sensor offset and scale factor corrections for the stable platform position pickoff signals.
Servo Compensation	Implement digital filters for servo stability compensators, integral compensation, resonance notch filters and torquer drive signal synthesis
Gyro Torquing	Process external commands to implement the platform rate command
Strapdown Alignment Processing	
Inertial Sensor Calculations	The inertial instruments outputs must be corrected for scale factor and bias errors. If multiple inertial instruments are used, they must be frequency blended to produce a composite output signal.
Coordinate Rotations	The tip-tilt axes of the inertial measurements must be rotated to match the corresponding tip-tilt axes of the alignment sensor. This rotation is dynamically dependent on the gimbal angle orientation, so the gimbal angle encoders must be processed to determine the correct rotation angle to apply.
Dynamic	Digital transfer function filters must be applied to

Compensation	dynamically match the inertial angle measure to the alignment loop transfer function in order to effect broadband correction.

Table 2 Comparison of Software Implementations Functions

The 4 system distinctions (stable platform, inertial instruments, alignment sensor and software) between the stabilized platform and strapdown beam control architectures have been presented in this section. The next section presents performance results for these architectures.

Performance Comparisons

Since the ultimate trade depends upon the capability of the strapdown to meet performance objectives, a straightforward strapdown mechanization was simulated to estimate the jitter performance that can be attained with such a system. The Matlab Simulink model is shown in Figure 14. First a jitter performance results for a strapdown configuration are presented for the low-amplitude space base motion environments. Then, jitter performance results for the more severe tactical base motion environment are presented for both the strapdown and stable platform architectures.

Evaluation

Only the base motion disturbances were modeled. Although sensor noise was not considered, it was taken into account for detailed performance studies. Sensors with suitable low-noise characteristics are believed to be available for this application, so the strapdown conclusions drawn here are not significantly altered by consideration of sensor noise. The three base motion sequences described in Figure 2 were simulated. These results are shown in Figures 15, 16, and17, and summarized in Table 3.

Case	BM Input [μRad]	Net Response [μRad]	Comments
1	53.	0.13	Low-Frequency Content

2	16.	0.15	Low-Frequency Content
3	15.	1.4	High-Frequency Content

Table 3. Summary of Strapdown Responses

The results tabulated above show that μradianฺ and sub-μradianฺ pointing performance is obtained, even with large base motion inputs. Note that the system performance of Case 1 is better than that of Case 2, even though the input disturbance is nearly 3 times larger, a relationship which occurs because of the difference in the frequency content of the two disturbance spectra. Note that the response in Case 3 is an order of magnitude larger than the error response of Case 2, even though the input disturbances have comparable rms values. Again, the larger error is due to the significantly larger high-frequency content of the Case 3 disturbance. These results show that suitable sub-μradianฺ performance is attainable with strapdown mechanizations. Furthermore, they show the sensitivity to high-frequency disturbance, where payload compliance (not modeled here) would contribute significantly to the already higher response. These effects would have to be carefully modeled to develop good performance predictions.

The results of the tactical base motion environment of Figure 3 are also simulated for both strapdown and stable platform configurations. These results, shown in Figure 18, show that only the stable platform configuration is viable for large-amplitude high frequency base motion environments. See in particular the direct comparison of the PSDs in Figure 19. The gyro measurement error comparison in Figure 20 shows that a strapdown configuration cannot possibly meet the precision accuracy requirements for this base motion environment. Figure 20

shows the gyro measurement error PSD for cases of 100, 500, and 1000 Hz gyro bandwidths. Tabulated in the plot are the corresponding gyro measurement error rms values. These cases correspond to the gimbal following error shown in Figure 18 for the strapdown system. The gimbals have pointing error (the 54- and 187-μradian error), which must be accurately measured by the gyros. These curves show that gyro bandwidths of 1.0 kHz or greater are required to measure the gimbal following motion with an error of less than a μradian. Of course, higher bandwidth instruments would be required with more severe gimbal following motion or for applications with more stringent pointing performance requirements.

This completes the jitter performance evaluation. Qualitative and cost comparisons are addressed next.

Qualitative

Table 4 compares the two jitter stabilization approaches qualitatively on the basis of 8 criteria. A "+" indicates the preferred implementation for each category. The table shows that the source probe beam requirements are the same in both implementations and that the other categories provide distinct preferences. The stabilized platform approach is favored in all categories except Component Count and the associated Failure Points. Due to its less demanding requirements on the inertial and alignment sensors, and on the software, the stabilized platform is the preferred configuration.

Category	Stabilized Platform	Strapdown
Component Count	-	+
Instrument Performance	+	-
Software Complexity	+	-
Electronics Complexity	+/-	-/+
Alignment Sensor	+	-
Probe Beam Source	Same	
Failure Points	-	+
Integration and Test Complexity	+	-

Table 4. Qualitative Comparisons

Cost

A qualitative cost analysis was performed. The major stabilized platform cost areas were identified and the fractional cost of each estimated. Then, the relative comparison of the corresponding strapdown system cost was estimated as a multiplier of the corresponding stabilized platform cost. These results were then computed to estimate a total development cost ratio between the stabilized platform and the strapdown implementations. This qualitative analysis shows that there is not a huge cost difference between the approaches. The strapdown configuration is estimated to cost approximately 15% less that the equivalent stabilized platform configuration. The inertial instrument and probe beam/sensor costs are believed to be comparable between the two mechanizations for this application. The platform associated costs are much less for the strapdown configuration. The platform cost attributed to the strapdown mechanization is not zero, however, to allow for the mechanical assembly and mounting of inertial instruments that is required. Similarly, the software development costs of implementing

the high-speed correction algorithms are believed to be roughly comparable to the software required to implement the stable platform. Finally, the integration costs of the strapdown mechanization are believed to be lower due to the reduced complexity of this approach.

Category	% of Platform Total Cost	Strapdown Weighting Factor	Strapdown Relative Cost
Gyros	11%	1.25	14%
Inertial Instruments	6%	1.00	6%
Platform Assembly (Including Sensors and Actuators)	9%	0.10	1%
Probe Beam	2%	1.00	2%
Alignment Sensor	6%	1.50	9%
Electronics	24%	1.25	30%
Software	24%	1.50	36%
Integration and Test	17%	1.25	22%
TOTAL	1		120%

Table 5 Qualitative Cost Comparisons

Conclusions

A quantitative and qualitative comparison of strapdown and stabilized platform approaches for broadband jitter control has been developed. For the base motion disturbance environment considered for the drivers of gimbal and pointing system requirements, data is shown to support the selection of the strapdown inertial stabilization approach. The strapdown inertial stabilization approach is shown to meet performance objectives, to have a simpler mechanization, and to have a lower cost for these applications.

Figure 21 shows the optical and control configurations alternatives of strapdown and stable platforms. It is clear to us that the stable platform approach offers the best jitter performance of these alternatives. The choice of a stable platform is dependent on the questions *Is it required to meet performance objectives?* and *Is it worth the additional cost?*

References

1. *Enhanced Precision Pointing Jitter Suppression System*, J. Gilmore et. al., Draper Laboratory, Paper SPIE 4632-5, 2001.

Author Biographies

Dr. James E. Negro is a Boeing Technical Fellow at Boeing-SVS, Inc., Albuquerque, New Mexico, where he has worked since 1999. He heads up their Boston office. From 1977 to 1999, Dr. Negro worked at the Draper Laboratory, Cambridge, Massachusetts. Prior to joining Draper, he served in the U.S. Air Force. Throughout his career, Dr. Negro has been involved with the design, development, analysis, and testing of precision line-of-sight pointing controls for high energy laser and electro-optical sensor application.

Dr. Steve Griffin is the Enabling Technologies Enterprise Lead at Boeing SVS and a Boeing Technical Fellow. His technical tasks are focused on integrated modeling for directed energy and imaging systems. His areas of expertise include integrated optical/structural modeling, structural acoustics, vibration management, and smart structures. Prior to joining Boeing, as a civilian and military employee at AFRL, his responsibilities were split between deployable optical structures and launch vehicle environment mitigation with involvement as program manager, in-house researcher, and technical lead.

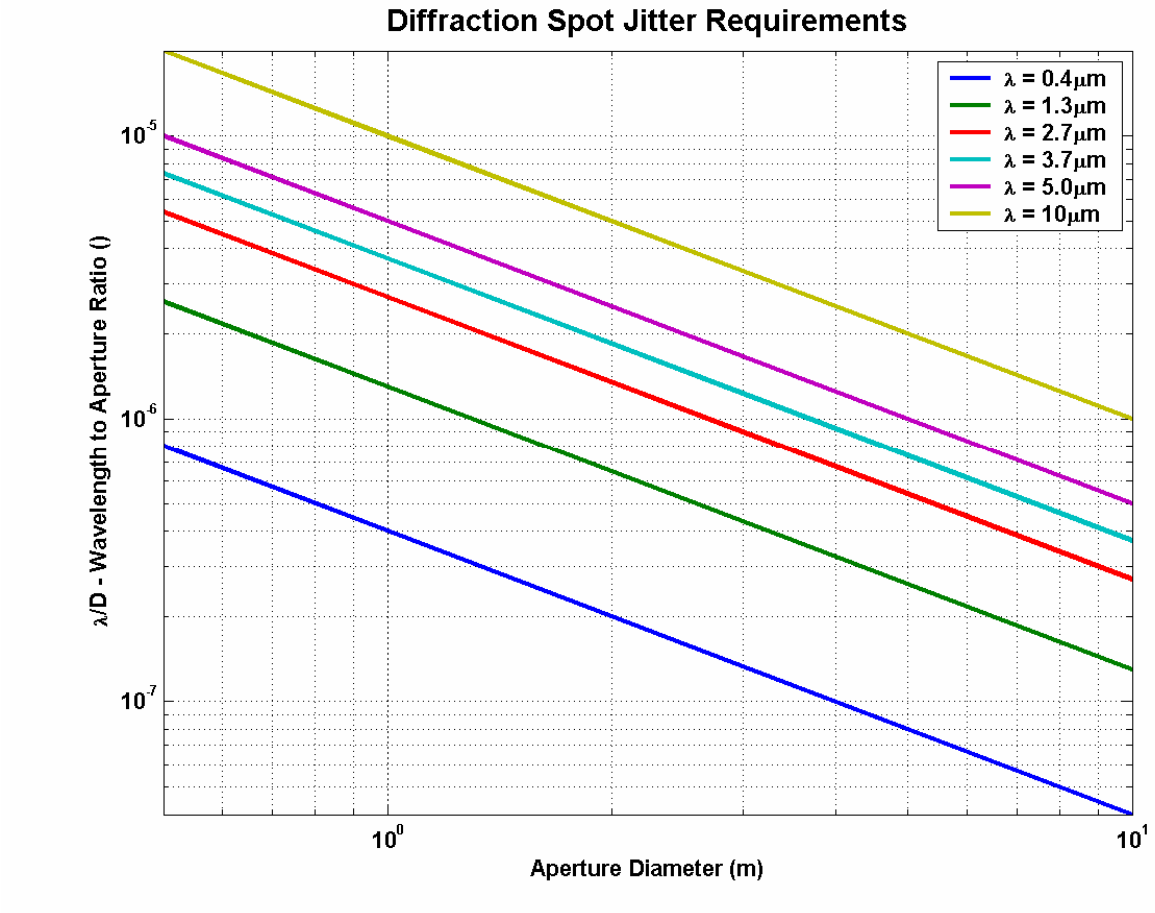

Figure 1 Nomograph showing λ/D ratios for hypothetical laser systems as a function of transmitting aperture diameter. The λ/D ratios are shown as a function of telescope diameter for a variety of laser wavelengths ranging from excimer lasers in the UV to CO2 lasers in the mid-IR. The aperture diameters range from a few tens of centimeters for terrestrial applications to 10 m for space applications. Required pointing accuracies scale directly with λ/D. LOS pointing accuracies range from approximately 20 μ radians for 50 cm CO2 laser systems (long wavelength; small aperture) to approximately 40 nanoradians for 10 m excimer laser systems (short wavelength; large aperture).

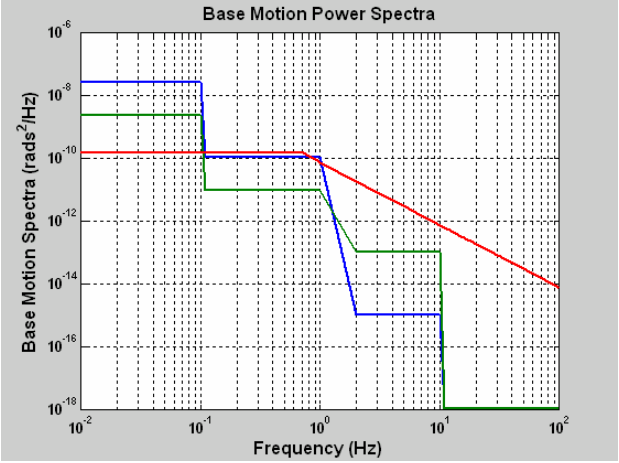

a) Power Spectral Density

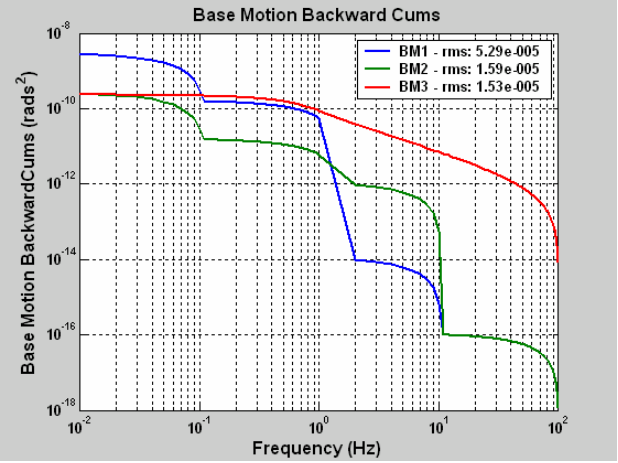

b) Backward Cumulative Power

Figure 2 Angle base motion disturbance vibration. Three distinct models are shown. These disturbance inputs are used for performance comparisons of the stabilized platform and strapdown jitter suppression systems. These spectra have base motion rms angles ranging from 15 to 53 μradians. These μradians are typical for satellite electro-optical pointing applications and also might represent a relatively quiet tactical application.

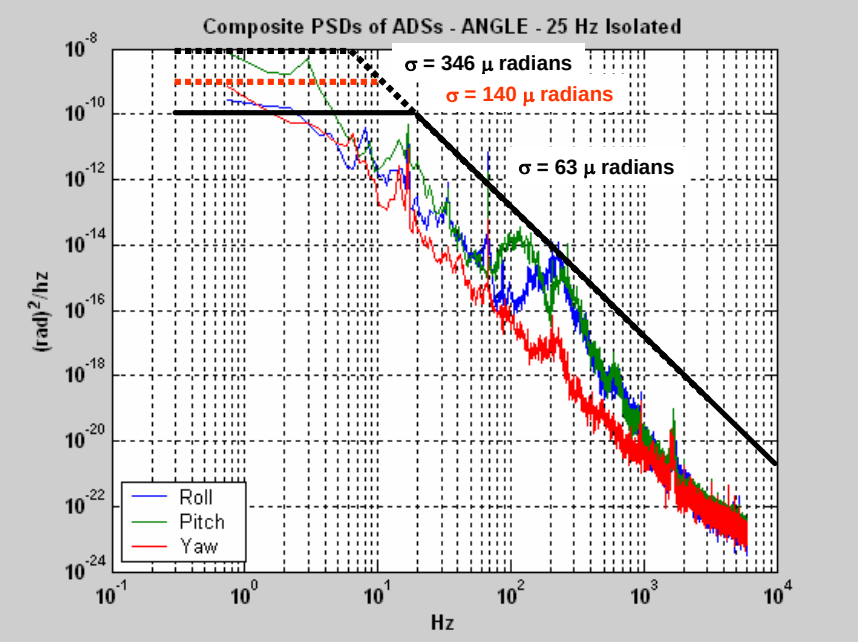

Figure 3 Tactical base motion angle spectra for the ASETS C-130 aircraft. Generally, tactical applications have a more severe base motion environment than a satellite application. The angular vibration measured for the ASETS C-130 aircraft is representative of a typical tactical environment, and is also used for performance comparisons of the stabilized platform and strapdown jitter suppression systems.

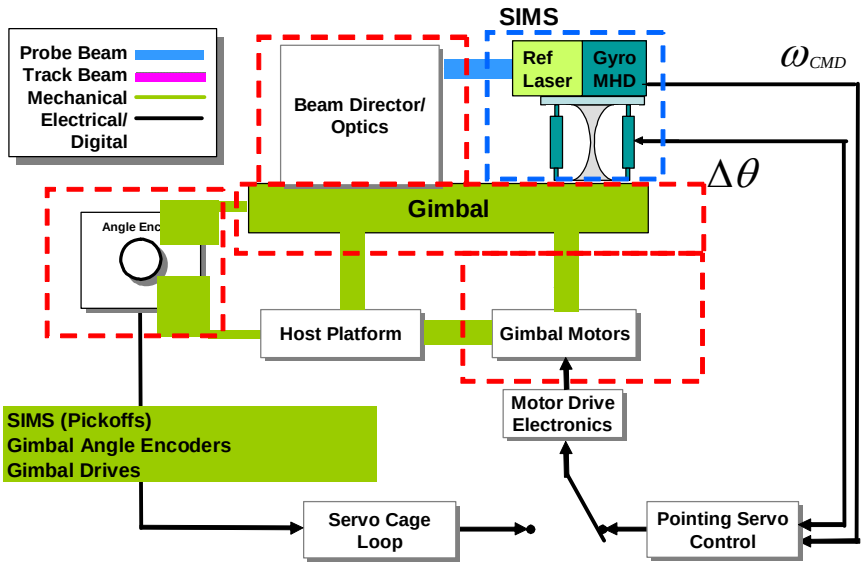

Figure 4 Stabilized inertial reference platform beam control architecture. This configuration is explicit for the case in which the beam director telescope is gimbaled with respect to a host platform. Another option might include a spacecraft pointing system as the gimbal.

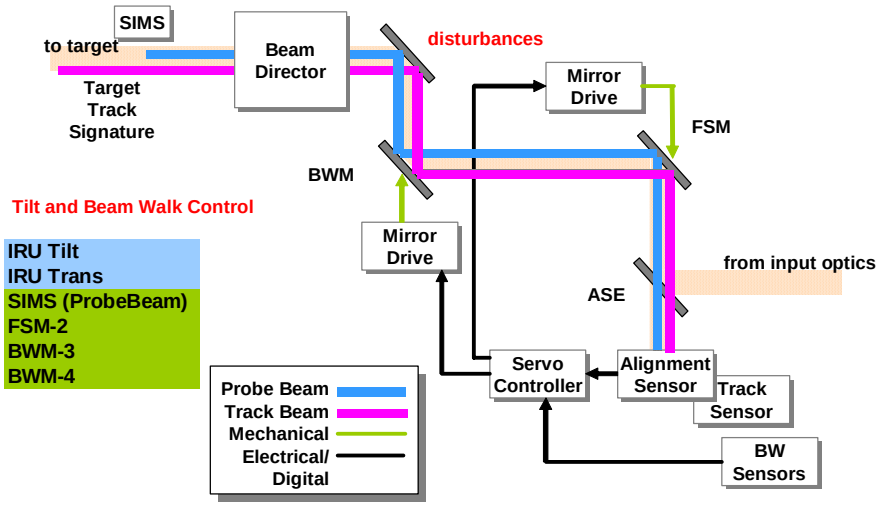

Figure 5 Beam train optical path alignment control loop. The optical path shows dual mirror actuators. A fast steering mirror controls jitter, while a beam walk mirror controls beam translation. Beam jitter and beam walk alignment sensors control these mirror actuators in a feedback servo control fashion.

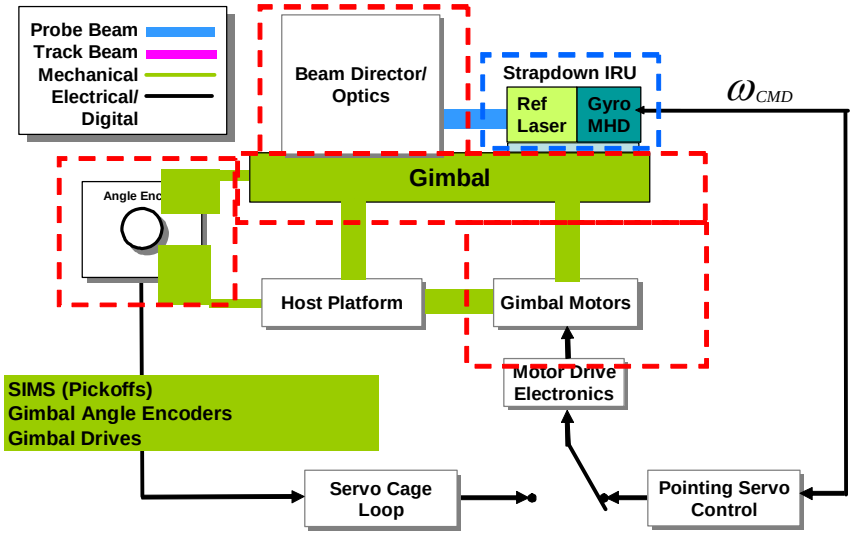

Figure 6 Strapdown stabilization beam control architecture. This configuration is explicit for the case in which the inertial angle sensors are strapped to the telescope. The gyro measured angular rate (or delta inertial angle) is used in an attitude computation to implement a telescope rate stabilization control loop.

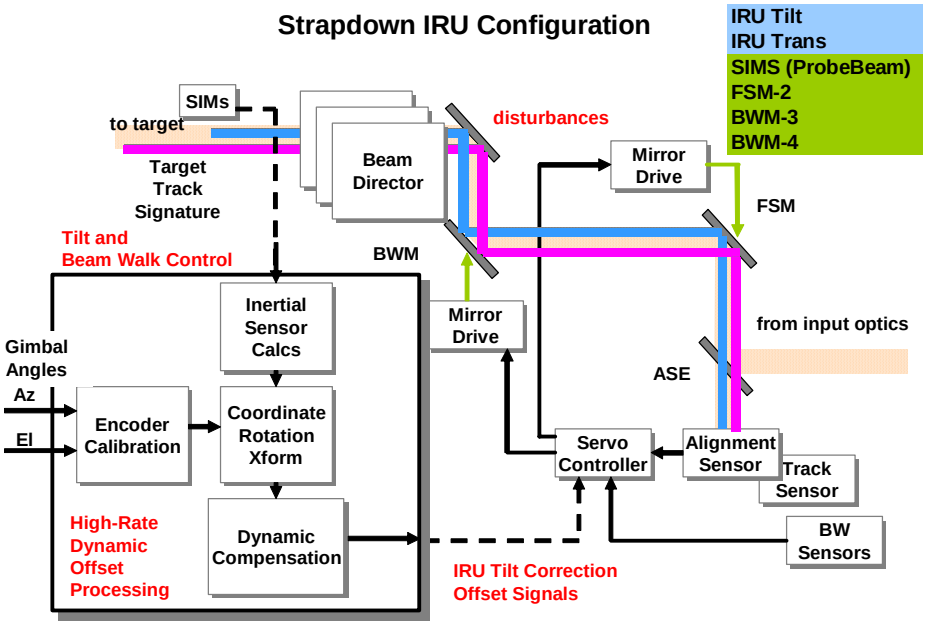

Figure 7 High-rate offset processing required for the strapdown implementation. The alignment system includes jitter alignment and beam walk sensors, just as it does for the stabilized platform mechanization. High-rate data processing is required to implement the calibration, and coordinate rotation and dynamic compensation computations for implementing the alignment system pointing offset. These angle offsets correct telescope pointing error.

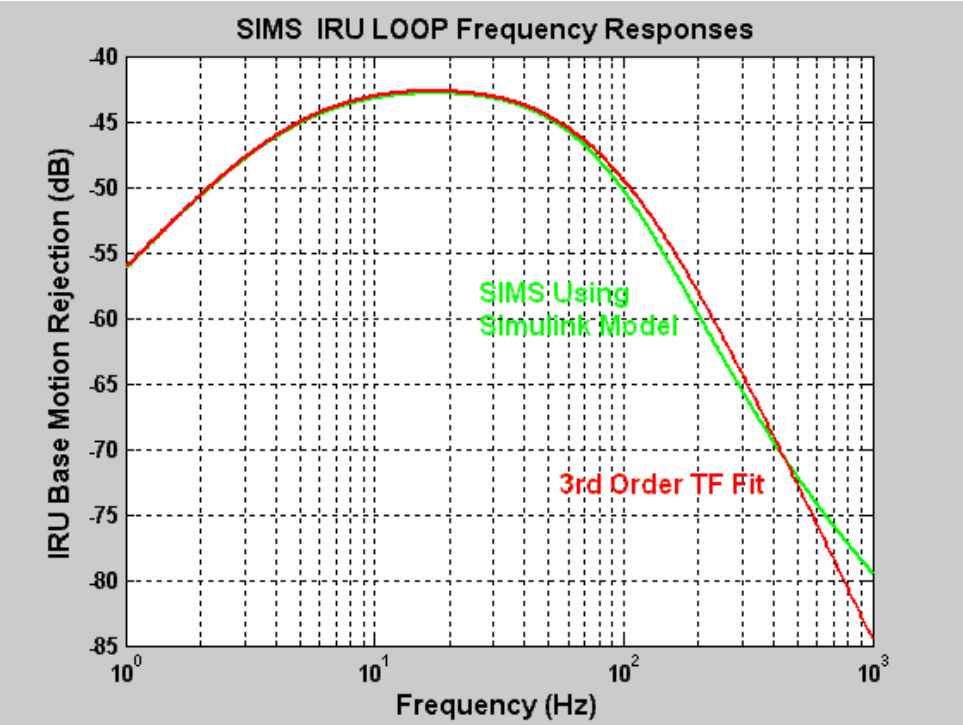

Figure 8 Stable platform base motion angle error rejection characteristics (red curve). Note that a minimum rejection of -42 dB is achieved. This transfer function, from base-motion input angle to platform angle, is typical of the base-motion error rejection characteristics typical of stabilized platforms.

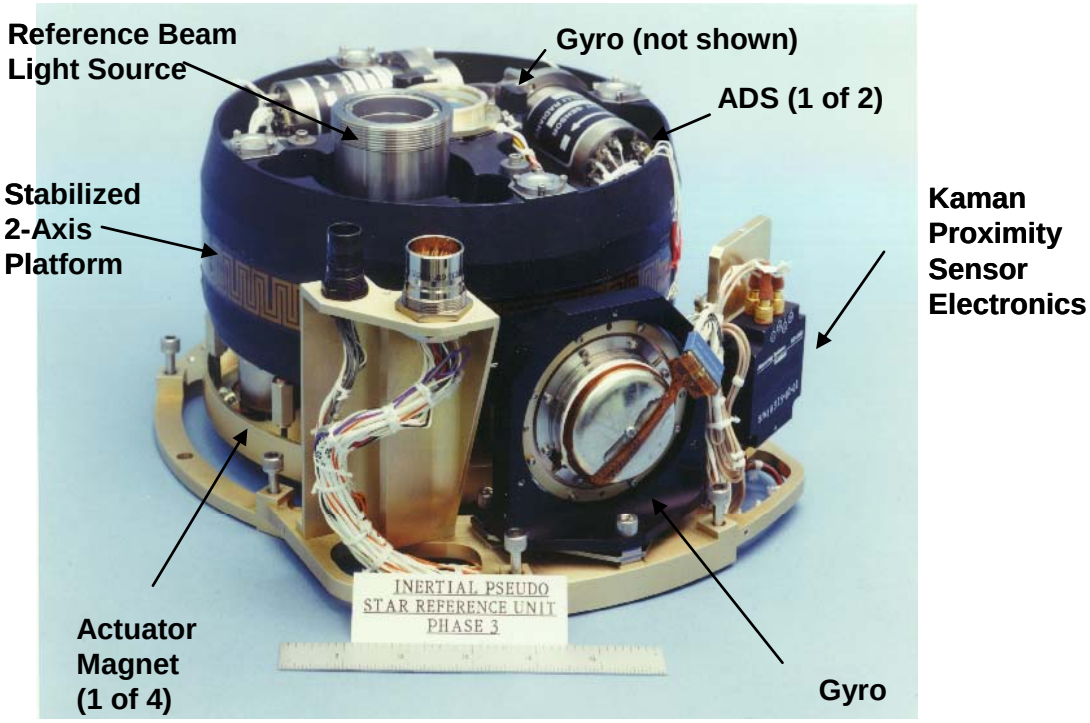

Figure 9 Inertial pseudo-reference unit built for MDA by the Draper Laboratory. A dry-tuned gyro the Singer-Kearfott MODIIe/s is used in the IPSRU, the most precise inertial stabilization system built to date.

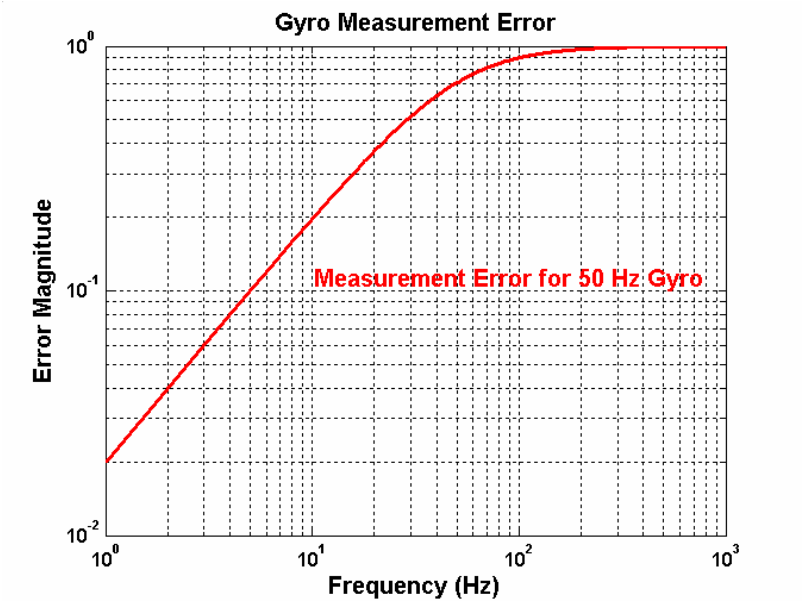

Figure 10 Gyro measurement error [magnitude of difference between gyro output and true inertial rate for a 50 Hz gyro bandwidth]. This magnitude is an important consideration for dynamic scale factor match in strapdown beam control configurations.

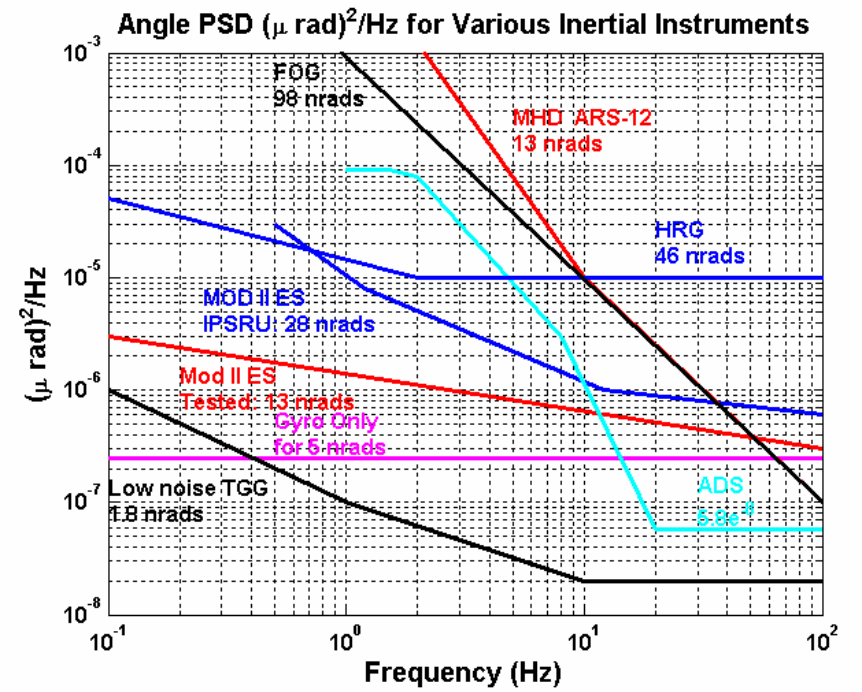

Figure 11 Inertial instrument spectra adapted from *Enhanced Precision Pointing Jitter Suppression System*. The noise spectra shown represents limits on performance on devices that use these inertial instruments. This data represents direct measurements obtained by the Draper Laboratory.

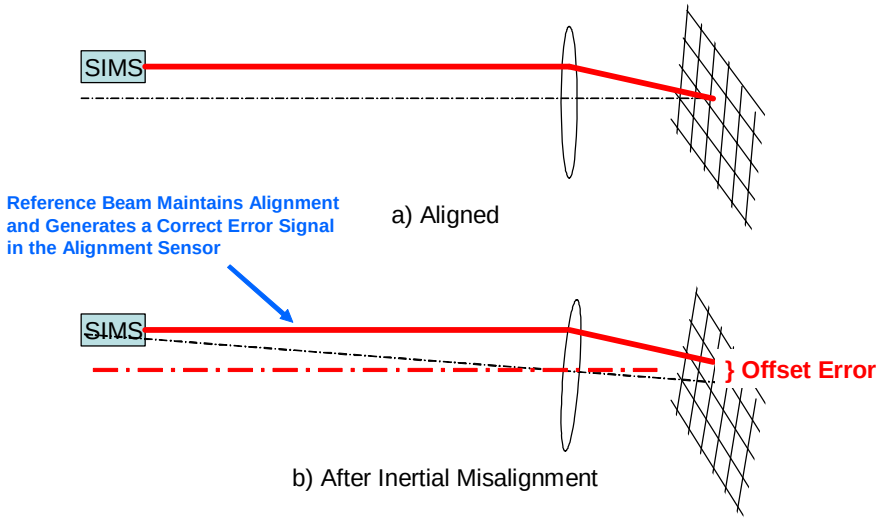

Figure 12 Alignment error sensor operation for stabilized platform implementations. In the stabilized platform case, the inertial motion of the telescope does not cause a stable platform error, because the platform is actively stabilized. This alignment error is sensed by the alignment probe beam sensor and corrected at high bandwidth.

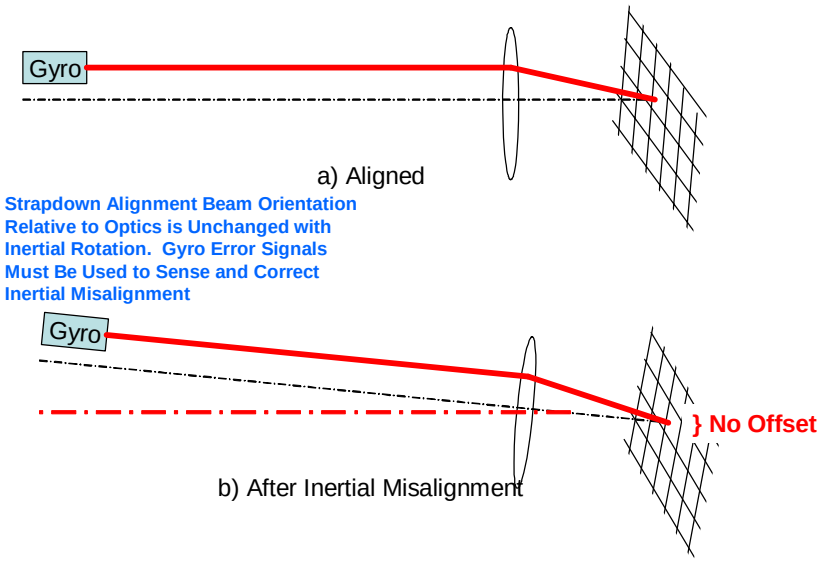

Figure 13 Alignment error sensor operation for strapdown implementations. In the strapdown case, inertial motion of the telescope moves the strapdown instruments, thereby generating an inertial angle error. However, there is no corresponding alignment error. The inertial angle sensors, by means of gimbal control, will act to minimize the pointing error, subject to the bandwidth limitations of the gimbal servo. Since the gimbal bandwidth is generally low in comparison to the disturbance induced error, a high effective bandwidth control must be used. This ((((()))is achieved by using the measured inertial angle error from the strapdown inertial sensors to offset the alignment servo in order to correct the overall beam pointing error induced by the telescope motion.

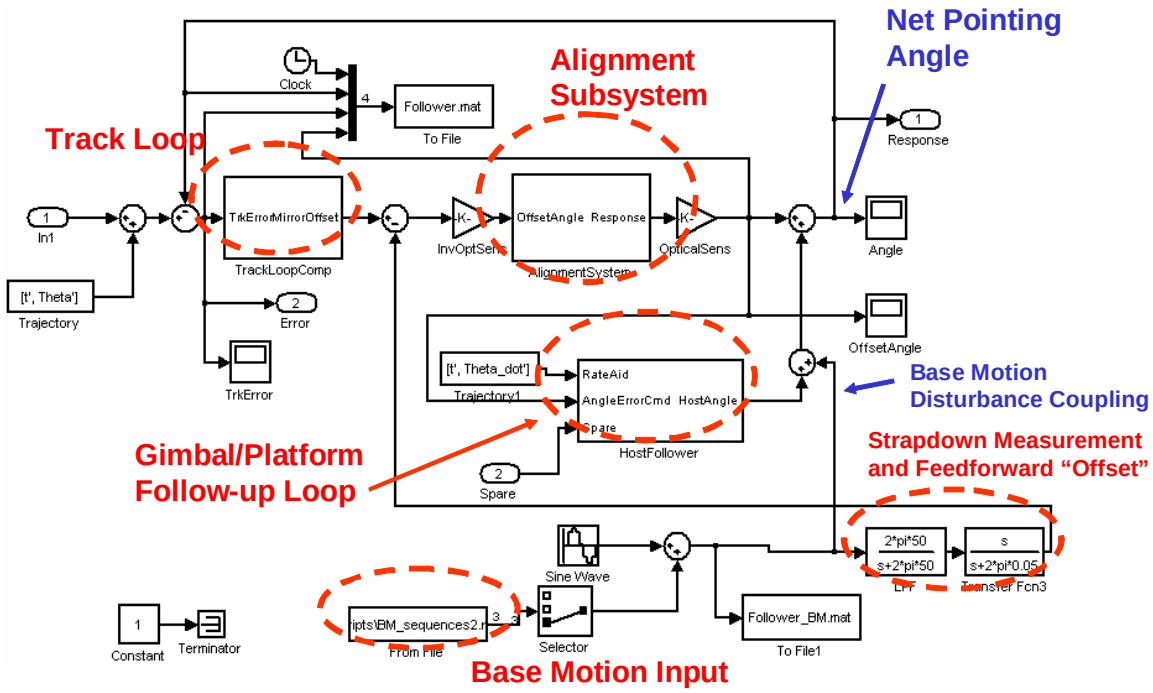

Figure 14 Matlab Simulink block diagram for a strapdown mechanization simulation. Since the ultimate trade depends on the capability of the strapdown to meet performance objectives, a straightforward strapdown mechanization was simulated to estimate the jitter performance that can be attained with such a system.

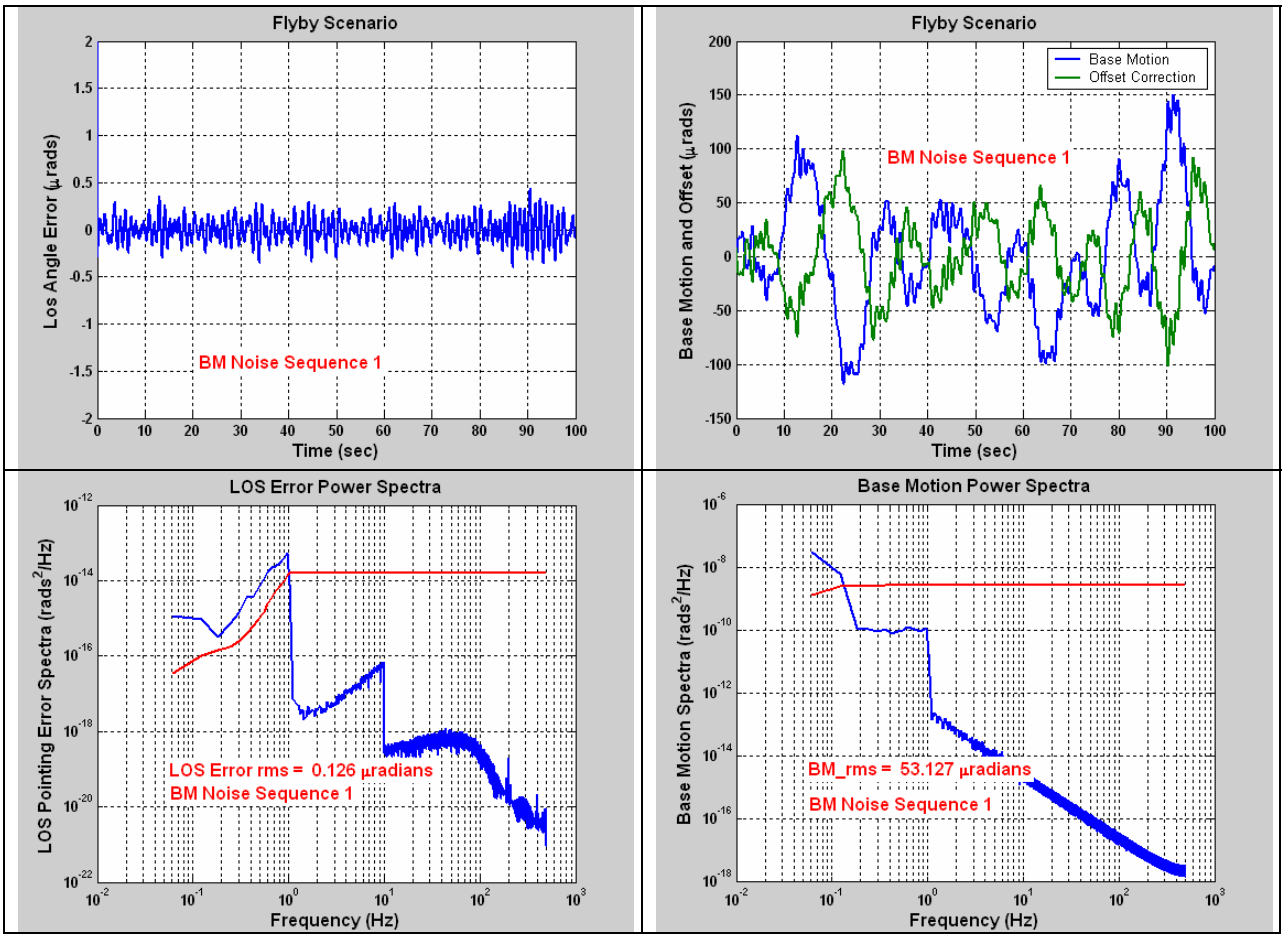

Figure 15 Strapdown configuration responses for angular disturbance base motion sequence 1 from Figure 2. For a base motion spectra of 53.1 μradians rms the resulting line-of-sight error is calculated at .126 μradians rms. The base motion sequence 1 has most of its energy content at relatively low frequencies.

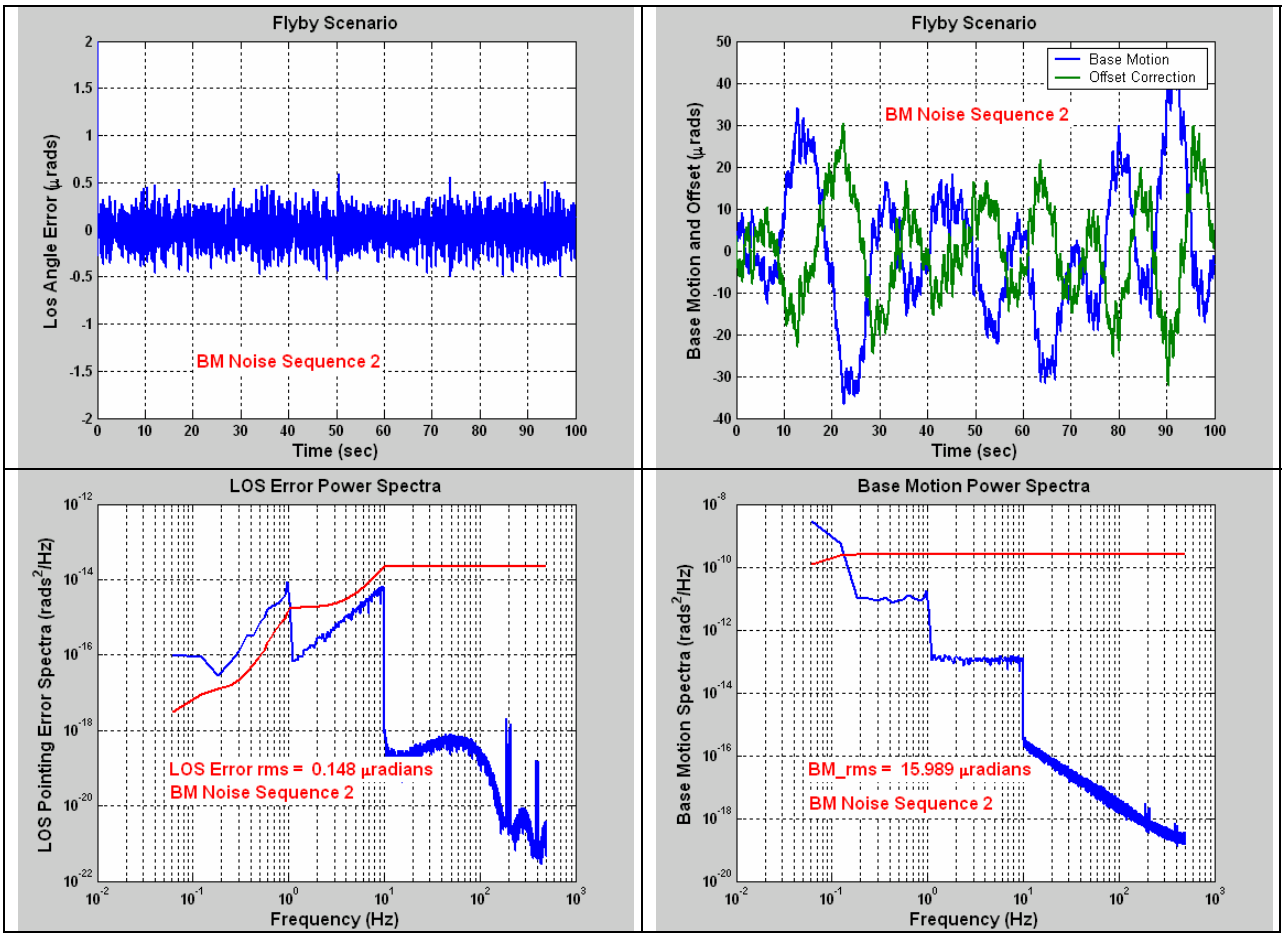

Figure 16 Strapdown configuration responses for angular disturbance base motion sequence 2 from Figure 2. For a base motion spectra of 16.0 μradians rms the resulting line-of-sight error is calculated at .148 μradians rms. Base motion sequence 2 has a lower rms magnitude than sequence 1 but has more energy at high frequencies, resulting in a slightly higher line-of-sight error.

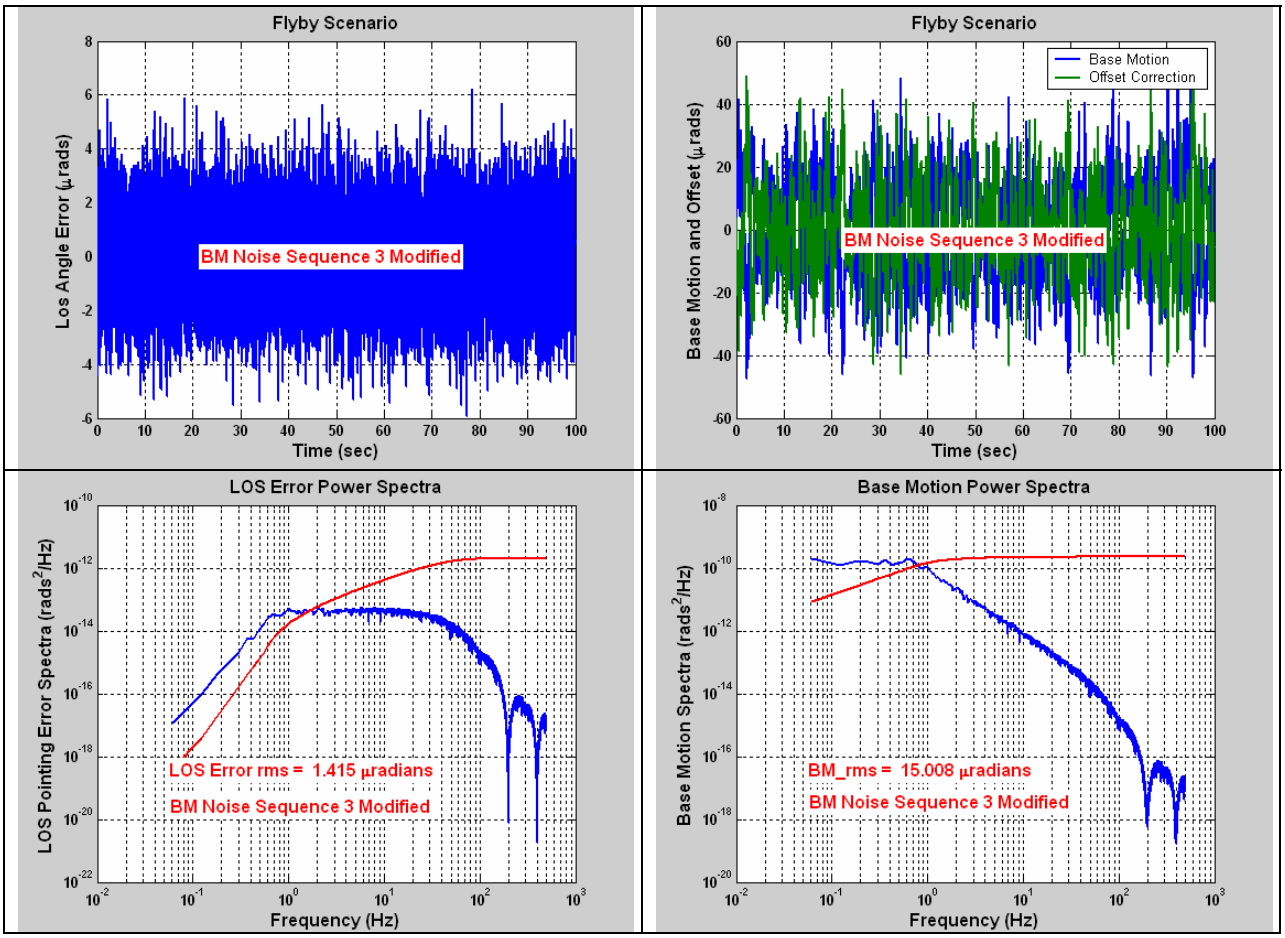

Figure 17 Strapdown configuration responses for angular disturbance base motion sequence 3 from Figure 2. For a base motion spectra of 15.0 μradians rms the resulting line-of-sight error is calculated at 1.42 μradians rms. Base motion sequence 3 has a significantly lower rms magnitude than sequence 1 and slightly lower than sequence 2. However, it has the highest line-of-sight error due to the highest magnitude of energy at high frequencies.

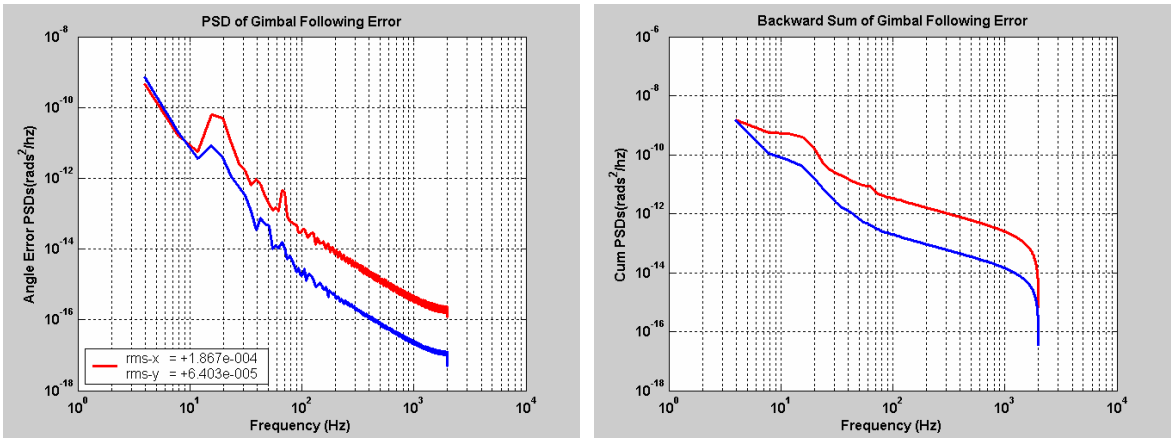

(a)

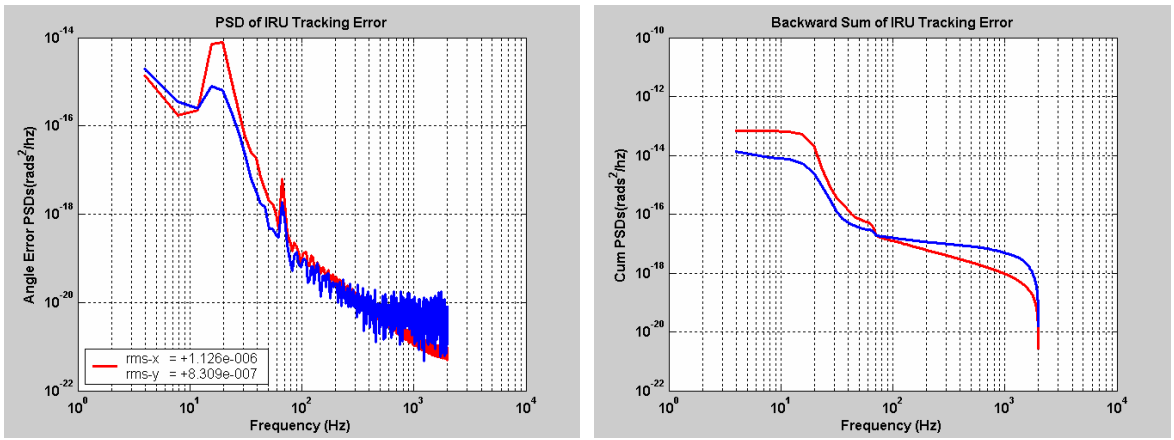

(b)

Figure 18 (a) Strapdown and (b) IRU stable platform gimbal following errors (PSD and backward sums: Tip-Tilt for the tactical base motion environment of Figure 3. These results clearly show that only the stable platform configuration is viable for large amplitude high frequency base motion environments.

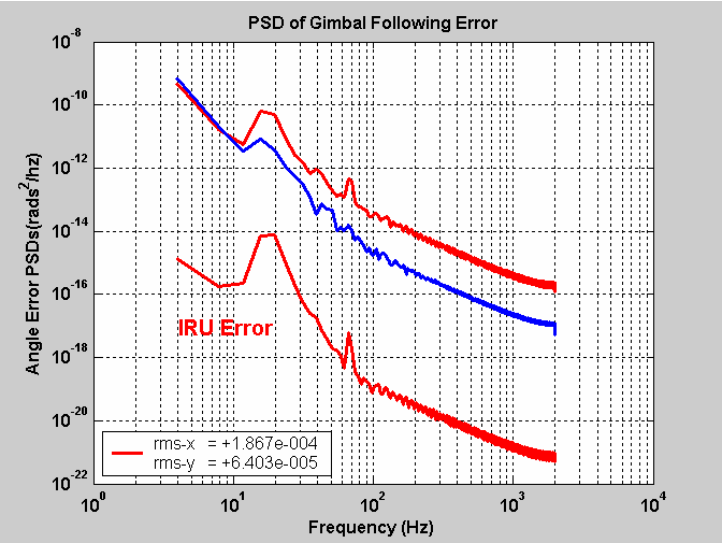

Figure 19 Direct comparison of the gimbal strapdown and IRU stable platform errors from Figure 18 for the tactical base motion case.

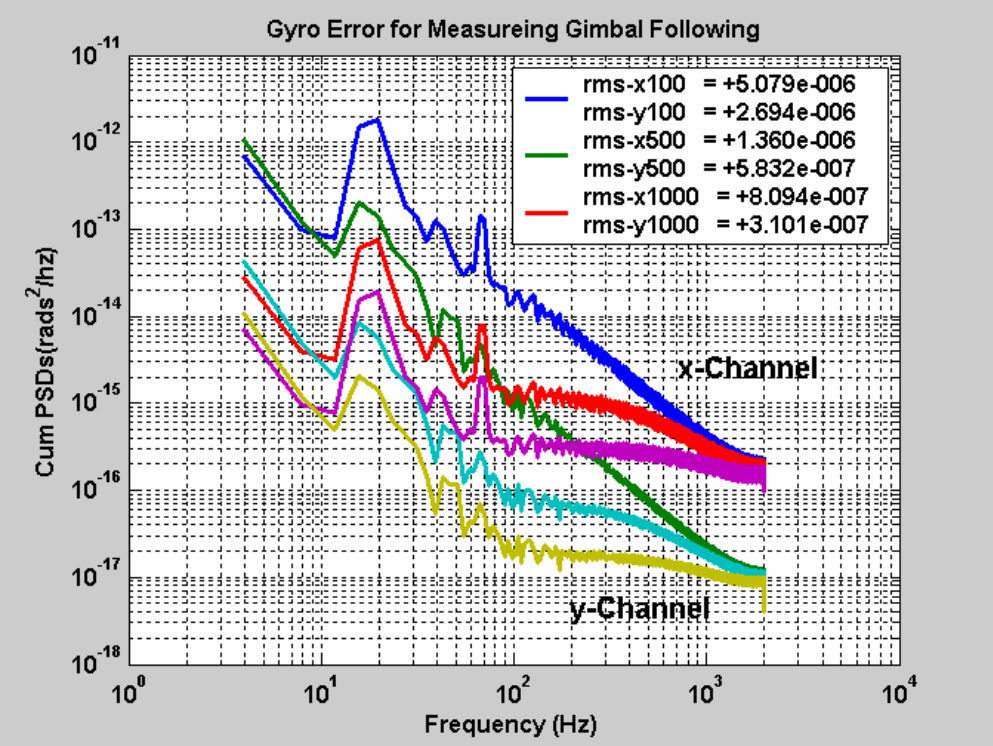

Figure 20 Gyro error variations with bandwidth for the strapdown configuration in the tactical base motion environment. The gyro measurement error comparison clearly shows that a strapdown configuration cannot possibly meet the precision accuracy requirements for this base motion environment. The gyro measurement error PSD is shown for cases of 100, 500 and 1000 Hz gyro bandwidths.

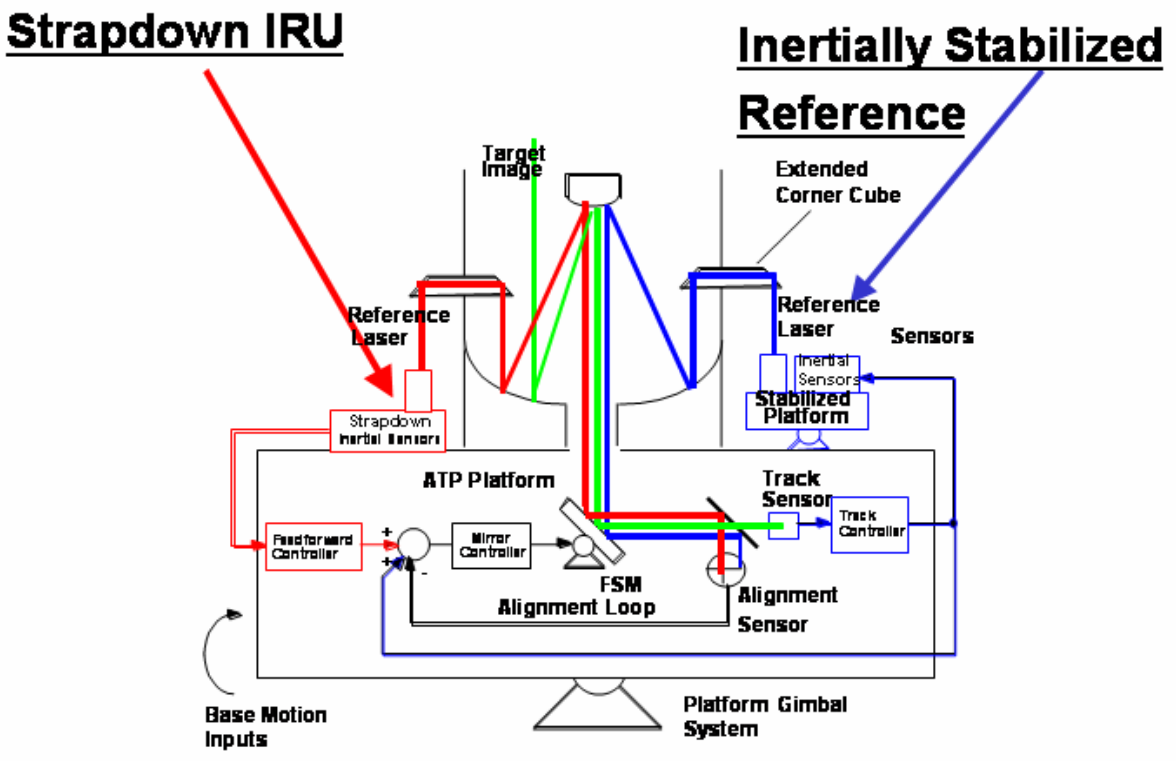

Figure 21 Comparative diagram: strapdown –vs- stabilized implementation trades. This diagram illustrates the optical and control configurations alternatives of strapdown and stable platforms.